Chinese Chemical Letters 35 (2024) 109265

Contents lists available at ScienceDirect

Chinese Chemical Letters

journal homepage: www.elsevier.com/locate/cclet

Highly polar CoP/Co_2P heterojunction composite as efficient cathode electrocatalyst for Li-air battery

Miaomiao Li[a], Mengwei Yuan[a,c], Xingzi Zheng[a], Kunyu Han[a], Genban Sun[a], Fujun Li[b], Huifeng Li[a,*]

[a] Beijing Key Laboratory of Energy Conversion and Storage Materials, College of Chemistry, Beijing Normal University, Beijing 100875, China
[b] Key Laboratory of Advanced Energy Materials Chemistry (Ministry of Education), College of Chemistry, Nankai University, Tianjin 300071, China
[c] Center for Advanced Materials Research, Beijing Normal University, Zhuhai 519087, China

ARTICLE INFO

Article history:
Received 31 July 2023
Revised 3 October 2023
Accepted 31 October 2023
Available online 3 November 2023

Keywords:
Li-air battery
Cathode catalyst
CoP/Co_2P
Heterojunction structure
High polarity

ABSTRACT

In order to advance the commercialization of rechargeable Li-air batteries, it is of importance to explore cathode catalyst with efficient catalytic activity. Transition metal oxides have poor electrical conductivity, while cobalt phosphide has excellent electrical conductivity and large specific surface area. Nevertheless, its application in organic Li-air batteries has been much less studied, and the electrocatalytic activity desires to be further elevated. Here, CoP/Co_2P heterojunction composite with higher polarity was fabricated. The discharge product of high-polarity CoP/Co_2P had a new porous box-like morphology, which was easy to be decomposed and exposed more active sites. The highly polar CoP/Co_2P heterostructure composite had homogeneous pores, the synergistic effect existed between CoP and Co_2P, and the discharge product was porous box mixed with Li_2O_2 and LiOH, which made CoP/Co_2P achieve high specific capacity of 14632 mAh/g and cycle stably 161 times when used as air electrode cathode catalyst. This work furnished a thought for the construction of cathode catalysts with efficient catalytic activity for Li-air batteries.

Much work is currently focused on electrochemical energy storage and conversion technologies in order to help energy technology innovation as well as development [1]. Li-air batteries have theoretically high energy density (≈ 3500 Wh/kg) [2], even comparable to gasoline, and are expected to be a potential alternative to scale energy storage and power batteries. However, lithium anode faced many challenges, such as formation of lithium dendrites and drastic volume changes. In this regard, researchers went deeper and made some progress [3,4]. For the cathode, the insulation of insoluble discharge product Li_2O_2 and the sluggish kinetics of gas-liquid-solid three-phase cathode reaction have led to high overpotential, low energy efficiency, limited cycling stability and poor multiplier performance, hindering the commercialization of Li-air batteries [5–7]. Catalysts can improve the slow kinetics of oxygen reduction reaction (ORR) [8,9] and oxygen evolution reaction (OER) [10–13], and improve the performance parameters. Developing stable and high-activity cathode catalysts is the key to improving the performance of Li-air battery. The effective catalytic activity and low price of transition metal oxides have captivated many researchers [14], while the poor electrical conductivity limits their commercialization [15]. Transition metal phosphides have excellent metal-like electronic conductivity and electrocatalytic activity, and have been utilized in a wide range of electrocatalytic reactions [16–18]. Among the many phosphides, cobalt phosphide has attracted much attention for its excellent electrical conductivity and large specific surface area. Cobalt phosphide has a variety of measurements, and CoP [19–21] or Co_2P is a popular research target at present. However, their electrocatalytic activity in organic Li-air batteries has been less studied. Related studies have shown that both CoP and Co_2P are worth investigating but the electrocatalytic activity desires to be further elevated.

LiOH-based batteries are more resistant to steam and more practical than Li_2O_2. The formation/decomposition of LiOH has been considered as a promising alternative pathway for the Li_2O_2 cycle [22]. To generate LiOH discharge products, we constructed CoP/Co_2P starting from high polarity. As cathode catalyst for Li-air battery, CoP/Co_2P composite could decrease the overpotential, increase the discharge capacity (14,632 mAh/g), and cycle stably up to 161 times, which was better than single CoP and Co_2P. The superior catalytic performance of CoP/Co_2P could be assigned to three reasons: (1) The extraordinary synergistic effect of the CoP/Co_2P heterojunction could modulate the electron density of cobalt metal and accelerate the electron transfer rate [23]; (2) The discharge

* Corresponding author.
E-mail address: lihuifeng@bnu.edu.cn (H. Li).

https://doi.org/10.1016/j.cclet.2023.109265
1001-8417/

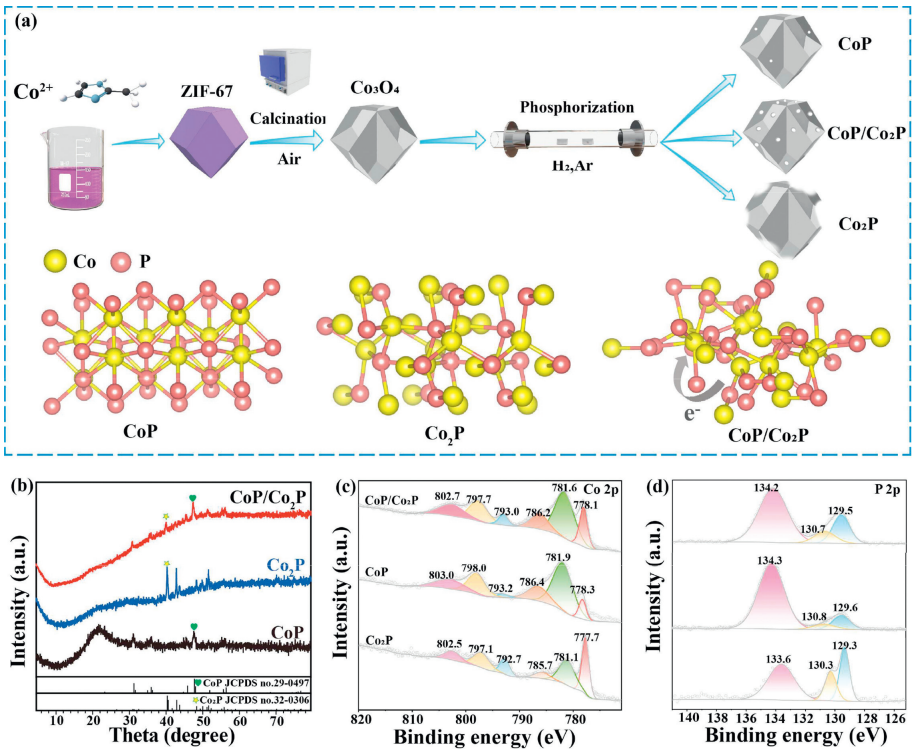

Fig. 1. (a) Scheme of preparation and micro-schematics of CoP, CoP/Co_2P and Co_2P. (b) XRD patterns of CoP, Co_2P and CoP/Co_2P heterojunction composite; The XPS results of (c) Co 2p, (d) P 2p of CoP, Co_2P and CoP/Co_2P heterojunction composite.

product was porous box of mixed LiOH and Li_2O_2, which facilitated the catalytic reactivity of OER/ORR; (3) the polyhedral skeleton was porous and stable. For the first time, we have studied the effects of CoP/Co_2P heterostructure composite on morphology of discharge products and performance of Li-air batteries from both catalyst composition and structural modulation, providing an idea for the design of metal phosphide cathode materials in Li-air batteries.

ZIF-67 was used as polyhedron template and Co_3O_4 was obtained by calcination in air. $NaH_2PO_2{\cdot}H_2O$ was then used as phosphorus source, and the phosphorylation temperature and the mass ratio of $NaH_2PO_2{\cdot}H_2O$ to Co_3O_4 were controlled to achieve controlled preparation of CoP/Co_2P. The preparing process was illustrated in Fig. 1a. According to the micro-schematics, we found that the polarity of CoP/Co_2P was higher than that of CoP or Co_2P.

The structure of the crystals was identified by X-ray diffraction (XRD). Fig. 1b exhibited the XRD spectra of CoP/Co_2P, CoP and Co_2P. The seven diffraction peaks at $2\theta = 35.0°$, 36.0°, 45.9°, 47.8°, 52.0°, 55.7° and 56.4° were considered to the (200), (111), (112), (211), (103), (020) and (301) crystalline planes of CoP (PDF #29–0497) [24]. Additional diffraction peaks were showed at 40.4°, 43.0°, 43.7° and 51.7°, which could be indexed to the (121), (211), (130) and (002) crystal planes of Co_2P (PDF #32–0306) [25], respectively. It was found that all the characteristic peaks shifted to a small angle due to the formation of heterojunction, which was consistent with the TEM results [26]. The above outcomes confirmed the successful synthesis of CoP/Co_2P heterojunction composite. CoP and Co_2P matched with standard cards JCPDS No. 29–0497 and JCPDS No. 32–0306, respectively, and no other peaks appeared. The XRD results indicated that the products changed from CoP to CoP/Co_2P and finally to Co_2P with the increase of phosphorylation temperature and the reduction of $NaH_2PO_2{\cdot}H_2O$ usage. Moreover, the elemental composition states and electron transfer behavior were characterized by X-ray photoelectron spectroscopy (XPS). In Fig. S1 (Supporting information), the surface of CoP/Co_2P was composed of Co, P and O elements. Fig. 1c showed that the Co 2p spectrum of CoP/Co_2P showed two dominant peaks near 778.1 eV ($2p_{3/2}$) and 793.0 eV ($2p_{1/2}$), belonging to the Co-P bond. In the meantime, two double peaks near 781.6/786.2 and 797.7/802.7 eV were assigned to the Co-O bond and the satellite peak, respectively [24,27–29]. The Co 2p spectra of CoP, Co_2P, and CoP/Co_2P showed analogous trends in the distribution of characteristic peaks. In CoP/Co_2P, the peaks of Co-P and Co-O bonds moved to lower binding energy than these of CoP, which indicated that the electron density of CoP had increased. Conversely, the peaks of CoP/Co_2P moved to higher binding energy than these of Co_2P, indicating a decrease in the electron density of Co_2P [24,30,31]. This result provided evidence for the large polarity of CoP/Co_2P. In the high-resolution P 2p (Fig. 1d), two peaks at 129.5 and 130.7 eV were attributed to Co-P bond of CoP/Co_2P and the peak at 133.9 eV was regarded as hypervalent P-species formed by surface oxidation that was inevitably exposed to air [29,32]. Compared with CoP and Co_2P, the shift patterns of the P 2p peaks of CoP/Co_2P were consistent with the above results, indicating strong electronic interactions between CoP and Co_2P, which could facilitate the adsorption of the target intermediates [33,34].

The morphology of ZIF-67, Co_3O_4, CoP/Co_2P, CoP, and Co_2P was studied by scanning electron microscopy (SEM). In Fig. 2a, ZIF-67 showed regular dodecahedra of approximately 500 nm in size. In Fig. 2b, when it was calcined in air, the polyhedral morphology was basically unchanged, and the smooth surface appeared depressed and wrinkled. In Fig. 2c, after further phosphate calcination, CoP/Co_2P showed uniform porous polyhedron with some wrinkles on the surface, and no collapse phenomenon was found. In addition, although CoP (Fig. S2a in Supporting information) was porous and polyhedral, the pore size and shape were not the same as CoP/Co_2P. The high temperature required to format Co_2P led to the occurrence of agglomeration and the absence of pores on the surface (Fig. S2c in Supporting information). To investigate the spatial structure of the porous polyhedron, further TEM studies

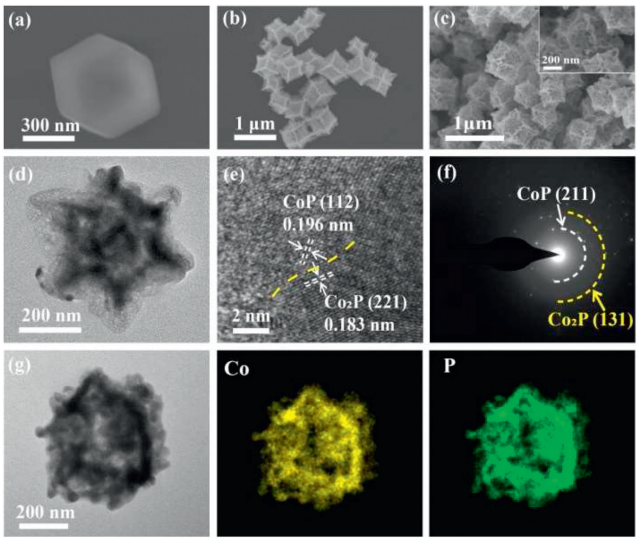

Fig. 2. SEM images of (a) ZIF-67, (b) Co_3O_4, (c) CoP/Co_2P (The inset was the corresponding enlarged SEM image). (d) The TEM, (e) HRTEM images, (f) SAED pattern and (g) element mapping of CoP/Co_2P heterojunction composite.

were carried out. In Fig. 2d, it was found that CoP/Co_2P was regular polyhedral morphology with some pores. Clear lattice stripes were observed from the HRTEM (Fig. 2e), where 0.196 nm spacing was corresponded to the (112) crystallographic plane of CoP and 0.183 nm spacing was corresponded to the (221) crystallographic plane of Co_2P. In addition, HRTEM studies in several ranges could reveal a clear and distinct boundary between CoP and Co_2P (Fig. S2e in Supporting information), indicating that CoP/Co_2P was heterogeneous structure. This was in consistency with the selected area electron diffraction (SAED) results (Fig. 2f). The elemental mapping results of CoP/Co_2P showed that both Co and P elements were homogenously represented in the polyhedral (Fig. 2g).

Fig. 3a showed a schematic of the first discharge capacity of CoP/Co_2P, CoP and Co_2P based Li-air batteries at 100 mA/g. CoP/Co_2P had the highest first-turn discharge specific capacity (14,632 mAh/g), much higher than Co_2P (6065 mAh/g) and CoP (10,208 mAh/g). During discharge, the CoP/Co_2P electrode had the highest discharge voltage plateau. The electrochemical impedance spectra (EIS) of the three catalysts were shown in Fig. 3b. The state density of Co_2P at the Fermi level was higher than that of Co_xP ($0<x<2$), which could promote the electron transfer and the adsorption of intermediates in the catalytic process [35], showing the smallest circular semicircle. As shown in Table S1 (Supporting information), the charge transfer resistance ($R_{ct}=66.23\ \Omega$) of CoP/Co_2P cathode was close to that of Co_2P ($R_{ct}=64.253\ \Omega$) and significantly lower than that of CoP ($R_{ct}=118.977\ \Omega$). This indicated that CoP/Co_2P heterojunction had higher electrical conductivity and lower charge transfer resistance, which was conducive to charge transfer and electron transport during the reaction of Li-air batteries. Fig. 3c showed CV curves for different catalysts under oxygen atmosphere with a scan range of 2.0–4.5 V and a scan rate of 5 mV/s. During the ORR process, the reduction peak around 2.50 V could be ascribed to Li_2O_2 and the peak current of CoP/Co_2P was significantly higher than CoP or Co_2P, suggesting that CoP/Co_2P had superior catalytic activity for ORR. During the OER, two typical reaction peaks were found at 3.30 and 4.25 V,

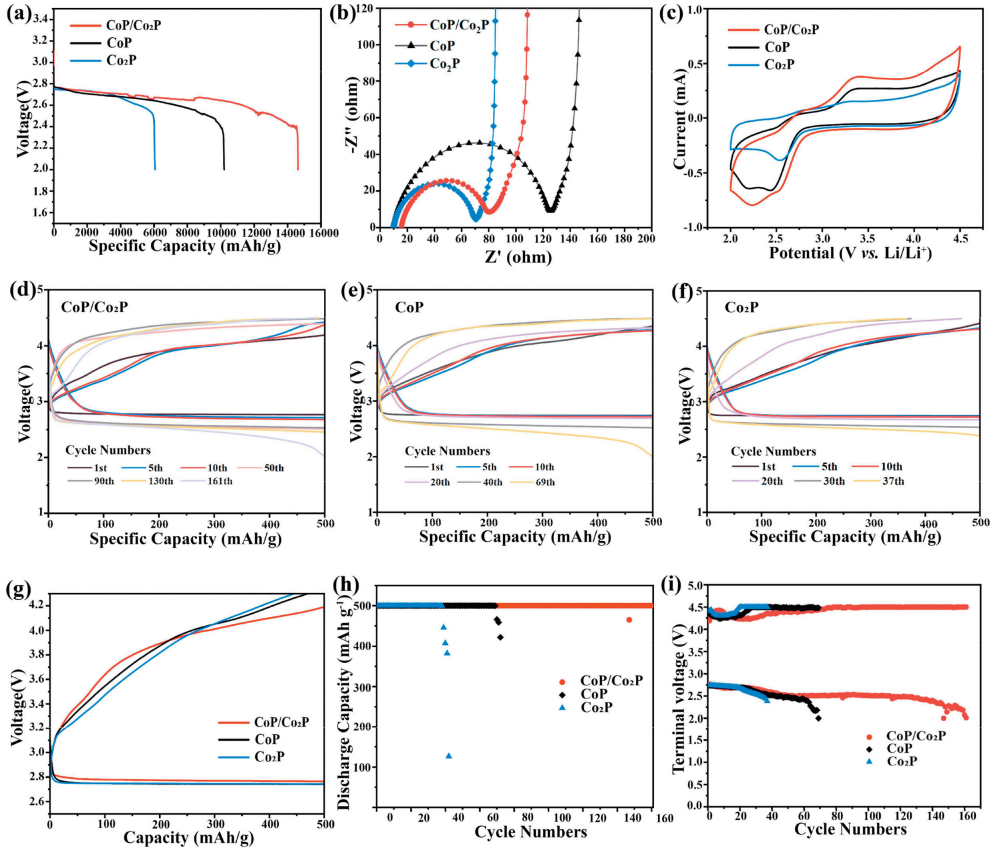

Fig. 3. (a) The first discharge curves for CoP/Co_2P, CoP and Co_2P cathodes at 100 mA/g. (b) EIS of different electrocatalysts. (c) CV curves at a scan range of 2.0–4.5 V and a scan rate of 5 mV/s. Charge and discharge curves for (d) CoP/Co_2P, (e) CoP and (f) Co_2P cathodes (200 mA/g, 500 mAh/g). (g) The 1st cycle discharge-charge curves (200 mA/g, 500 mAh/g). (h) The variation of the termination voltage with the number of cycles. (i) Cycle performance chart (200 mA/g, 500 mAh/g).

Table 1
Comparison of electrochemical performance between this work and a few reported cobalt phosphate cathodes.

Catalysts materials	Current density (mA/g)	Cycle number (cycles)	Morphology of Li_2O_2
Co_2P/Ru/CNT	100	185	Nanosheets stacking [36]
Co_2P/AB	0.1 mA/cm^2	132	Toroidal shape [37]
CoP/$Ti_3C_2T_x$	500	40	Flower-like shape [21]
$CoMoP_2$@NPC	100	102	Toroidal shape [38]
This work	200	161	Porous box

which were attributed to Li^+ stripping from the outer surface of Li_2O_2 and the oxidation of Li_2O_2 or by-product decomposition, respectively. The response current for CoP/Co_2P were the highest, indicating higher OER catalytic activity.

The specific capacity of battery discharge was limited to 500 mAh/g to alleviate the electrode polarization problem and to investigate the cycling stability of different cathodes. Fig. 3g showed the first charge/discharge curves of the CoP/Co_2P, CoP and Co_2P electrode Li-air batteries at 200 mA/g and 500 mAh/g. The CoP/Co_2P electrode showed the over-potential of 1.19 V, which was lower than that of both CoP (1.24 V) and Co_2P (1.21 V). As shown in Figs. 3d-f, the CoP/Co_2P electrode cycled steadily 161 cycles at 200 mA/g, while the CoP and Co_2P electrodes showed relatively limited cycling performance of 69 and 37 cycles, respectively. This conclusion was also obtained in Fig. 3h. This indicated that the formation of the high polarity heterojunction structure had greatly improved the cycling performance of the CoP/Co_2P electrode.

Fig. 3i showed the charge/discharge termination voltage for the CoP/Co_2P, CoP and Co_2P electrodes. It was clearly observed that CoP/Co_2P had the lowest charge/discharge overpotential, which cycled steadily 161 times and showed good cycle reversibility. For CoP or Co_2P, the number of cycles was limited and polarization occurred earlier. The results showed that the highly polar CoP/Co_2P heterostructure composite showed higher ORR and OER catalytic activity and better cycling stability during cell operation.

Table 1 compared the differences in electrochemical performance between this study and a few reported cobalt-based cathodes for Li-air batteries. By comparison, we found that CoP/Co_2P had excellent cycling performance and newly shaped discharge products.

To further research the effect of high-polarity heterostructure on the discharge products of Li-air batteries, the electrodes were further characterized by non-*in situ* XRD and SEM. Fig. 4a showed the XRD graphs of the three electrodes in pristine, discharge and recharge. After full discharge, all three electrodes showed distinct peaks at around 32.9°, 35.0° and 58.8°, coinciding with the (100), (101) and (110) crystallographic planes of Li_2O_2 (PDF#74-0115), respectively. The above results indicated that Li_2O_2 was the discharge product of CoP or Co_2P based Li-air battery, while the dominant discharge products of CoP/Co_2P were the mixture of Li_2O_2 and LiOH. The reasons for the formation of LiOH could be attributed to the following two items: (1) the presence of LiI in the TEDMG electrolyte acted as a driving force for the formation of LiOH [39]; (2) CoP/Co_2P was more polar than CoP or Co_2P and could adsorb enough water to form LiOH. Similar observation had been reported in Ag/δ-MnO_2 electrode [40]. Compared to Li_2O_2, which was susceptible to steam and carbon dioxide, Li-air batteries based on LiOH formation/decomposition had natural immunity to water and had better carbon dioxide tolerance, facilitating long cycle performance [41]. This was consistent with the result that CoP/Co_2P had the longest cycle life. When charged, the diffraction peaks of the discharge products disappeared and the XRD spectra of the electrode returned to their initial appearance, where the discharge products were effectively decomposed.

Figs. 4b–d were the SEM images of the three electrodes at each stage of charge and discharge. In Figs. 4b_1, c_1, d_1, CoP/Co_2P, CoP and Co_2P were able to maintain their original morphology. As shown in Figs. 4b_2, c_2, d_2, after discharging at 100 mA/g, the surface of each cathode was completely covered with discharge products, and the morphology of these discharge products was significantly different. As shown in Figs. 4b_3, c_3, d_3, after charging, the discharge products were effectively decomposed and the electrodes were restored to their original state. Typical toroidal discharge products were found at the surface of the CoP and Co_2P electrodes, where the diameter of the Co_2P discharge products (approximately 2.5 μm) was larger than that of CoP (1.1 μm). The shape and size of the discharge products had noteworthy effect on the performance of the Li-air batteries [42]. The smaller scale of the discharge product Li_2O_2, the easier it was to get sufficient decomposition during the following charging process. Therefore, the cycling stability of CoP was theoretically higher than Co_2P, which was in accordance with the actual cycling results. The morphology of the discharge products on the surface of CoP/Co_2P cathode was more distinct from that of the other two electrodes. The discharge products were a type of porous boxes, uniformly covering the electrode surface. The homogeneous and porous discharge products were easier to be decomposed, and the triple phase point of discharge products, electrolyte and catalyst facilitated OER catalytic activity. Additionally, the product morphology could reduce the adhesion area, expose more catalytic active sites, and increase

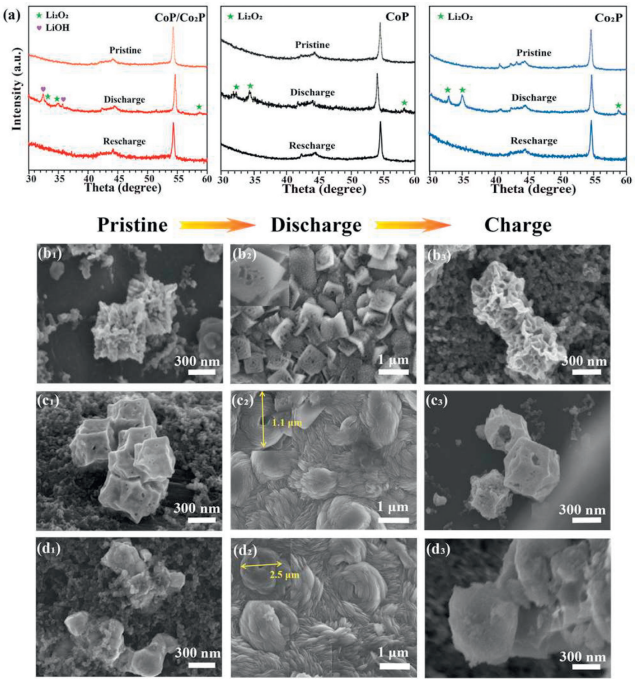

Fig. 4. (a) XRD photographs of CoP/Co_2P, CoP and Co_2P electrodes at various stages of charging and discharging; SEM images of CoP/Co_2P, CoP and Co_2P based cathodes under different charging and discharging states and the corresponding magnified SEM images (inset). (b_1, c_1, d_1) Primary cathode before discharge; (b_2, c_2, d_2) after the first discharge at 100 mA/g; (b_3, c_3, d_3) after first cycle charge.

the discharge capacity and ORR catalytic activity. The difference in the component and structure of cathode materials made the morphology of discharge products of Li-air batteries have such a big difference.

Through the above research, we found that the above properties could be attributed to three main features of the CoP/Co_2P structure. (1) CoP/Co_2P had higher polarity and could produce LiOH discharge products. Compared to Li_2O_2, LiOH-based Li-air batteries were naturally immune to water and air, with a theoretical capacity of 3707 Wh/kg (3505 Wh/kg for Li_2O_2-based Li-air batteries) [22]. The formation/decomposition of LiOH has been considered as a promising alternative pathway for the Li_2O_2 cycle; (2) CoP/Co_2P heterojunction had synergistic effect between multi-components, which could promote rapid interfacial charge transfer [43,44] and improve battery performance; (3) CoP/Co_2P presented porous polyhedral structure and rough and uneven surface, which facilitated electrolyte penetration and provided a large number of channels for the transport of ions and oxygen during the reaction process [44].

In conclusion, the highly polar CoP/Co_2P heterostructure composite were constructed by stirring combined calcination method and used as the cathode of Li-air battery. CoP could improve catalytic activity, and Co_2P could promote the electron transfer and intermediate adsorption during the catalytic process. Highly polar CoP/Co_2P heterostructure composite exhibited excellent capacity performance (14,632 mAh/g at 100 mA/g), which was result of the mixed Li_2O_2 and LiOH discharge products. Moreover, the CoP/Co_2P composite had synergistic effect, and the new porous box-like discharge products were easily disintegrated, resulting in a stable cycle of 161 times. CoP/Co_2P based Li-air battery showed lower overpotential, high specific capacity and high cycling stability, indicating that CoP/Co_2P composite had important research significance in the cathode catalyst of inert Li-air batteries.

Declaration of competing interest

The authors declare that they have no known competing financial interests or personal relationships that could have appeared to influence the work reported in this paper.

Acknowledgment

This work was supported by the National Science Foundations of China (Nos. 21871028, 22271018).

Supplementary materials

Supplementary material associated with this article can be found, in the online version, at doi:10.1016/j.cclet.2023.109265.

References

[1] M. Yuan, Z. Sun, H. Yang, et al., Energy Environ. Mater. 6 (2022) e12258.
[2] D. Cao, S. Zang, F. Yu, et al., Batteries Supercaps 2 (2019) 428–439.
[3] Y.S. Hong, C.Z. Zhao, Y. Xiao, et al., Batter. Supercaps 2 (2019) 638–658.
[4] X. Liu, Q. Zhang, Y. Ma, et al., J. Energy Chem. 69 (2022) 270–281.
[5] M. Li, M. Yuan, X. Zheng, et al., J. Beijing Norm. Univ. Nat. Sci. 59 (2023) 401–412.
[6] X. Zheng, M. Yuan, Y. Zhao, et al., Adv. Energy Mater. 13 (2023) 2204019.
[7] W.J. Kwak, D.S Rosy, et al., Chem. Rev. 120 (2020) 6626–6683.
[8] D. Wang, M. Yuan, J. Xu, et al., ACS Sustain. Chem. Eng. 9 (2021) 16956–16964.
[9] S. Gao, B. Fan, R. Feng, C. Ye, X. Wei, J. Liu, X. Bu, Nano Energy 40 (2017) 462–470.
[10] Z. Sun, L. Lin, C. Nan, et al., ACS Sustain. Chem. Eng. 6 (2018) 14257–14263.
[11] Z. Sun, M. Yuan, L. Lin, et al., Chem. Commun. 55 (2019) 9729–9732.
[12] L. Xia, J. Wang, L. Bo, et al., Chem. Eng. J. 467 (2023) 143464.
[13] L. Xia, L. Bo, W. Shi, et al., Chem. Eng. J. 452 (2023) 137250.
[14] Y. Cai, Y. Hou, Y. Lu, J. Chen, Inorganics 7 (2019) 69–94.
[15] B. Wang, Y. Ren, Y. Zhu, et al., Adv. Sci. 10 (2023) e2300860.
[16] H. Zhao, Z.Y. Yuan, Catal. Sci. Technol. 7 (2017) 330–347.
[17] M. Sun, H. Liu, J. Qu, J. Li, Adv. Energy Mater. 6 (2016) 1600087.
[18] J. Tong, W. Li, L. Bo, et al., Electrochim. Acta 320 (2019) 134579.
[19] Y. Zhang, W. Shi, L. Bo, et al., Chem. Eng. J. 431 (2022) 134188.
[20] J. Tong, Y. Li, L. Bo, et al., ACS Sustain. Chem. Eng. 7 (2019) 17432–17442.
[21] X. Zheng, M. Yuan, X. Huang, H. Li, G. Sun, Chin. Chem. Lett. 34 (2023) 107152.
[22] Z. Gao, I. Temprano, J. Lei, et al., Adv. Mater. 35 (2023) e2201384.
[23] Y. Zhu, X. Wu, Prog. Mater. Sci. 131 (2023) 101019.
[24] B. Liu, R. Wang, Y. Yao, et al., Chem. Eng. J. 431 (2022) 133228.
[25] X. Peng, Y. Liu, S. Hu, et al., J. Alloy. Compd. 889 (2021) 161628.
[26] X. Li, Q. Liu, F. Deng, et al., Appl. Catal. B: Environ. 314 (2022) 121502.
[27] K. Xu, H. Cheng, H. Lv, et al., Adv. Mater. 30 (2018) 1703322.
[28] M. Wang, M. Wang, Y. Fu, S. Shen, Chin. Chem. Lett. 28 (2017) 2207–2211.
[29] Z. Zhou, N. Mahmood, Y. Zhang, et al., J. Energy Chem. 26 (2017) 1223–1230.
[30] I. Krivtsov, E.I. García-López, G. Marcì, et al., Appl. Catal. B: Environ. 204 (2017) 430–439.
[31] D. Xu, T. Yang, Y. Dong, et al., Ceram. Int. 49 (2023) 16999–17007.
[32] X. Guo, X. Yu, Z. Feng, et al., ACS Sustain. Chem. Eng. 6 (2018) 8150–8158.
[33] T. Liu, D. Liu, F. Qu, et al., Adv. Energy Mater. 7 (2017) 1700020.
[34] Q. Xu, H. Jiang, H. Zhang, Y. Hu, C. Li, Appl. Catal. B: Environ. 242 (2019) 60–66.
[35] H. Liu, J. Guan, S. Yang, et al., Adv. Mater. 32 (2020) e2003649.
[36] P. Wang, C. Li, S. Dong, et al., Small 15 (2019) e1900001.
[37] H.B. Huang, S.H. Luo, C.L. Liu, T.F. Yi, Y.C. Zhai, ACS Appl. Mater. Interfaces 10 (2018) 21281–21290.
[38] H. Xu, L. Zhao, X. Liu, et al., FlatChem 25 (2021) 100221.
[39] W.J. Kwak, D. Hirshberg, D. Sharon, et al., J. Mater. Chem. A 3 (2015) 8855–8864.
[40] L. Dai, Q. Sun, Y. Yao, et al., Sci. China Mater. 65 (2022) 1431–1442.
[41] S.M. Cho, J.H. Yom, S.W. Hwang, et al., J. Power Sources 342 (2017) 427–434.
[42] E. Yilmaz, C. Yogi, K. Yamanaka, T. Ohta, H.R. Byon, Nano Lett. 13 (2013) 4679–4684.
[43] X. Han, Y. Liang, L. Zhao, et al., Mater. Futur. 1 (2022) 035102.
[44] X. Zheng, M. Yuan, D. Guo, et al., ACS Nano 16 (2022) 4487–4499.